Journal of Bioenergetics and Biomembranes, Vol. 27, No. 4, 1995

Structure–Function Relationships of the Alternative Oxidase of Plant Mitochondria: A Model of the Active Site

Anthony L. Moore,[1] Ann L. Umbach,[2] and James N. Siedow[2]

Received April 24, 1995

A major characteristic of plant mitochondria is the presence of a cyanide-insensitive alternative oxidase which catalyzes the reduction of oxygen to water. Current information on the properties of the oxidase is reviewed. Conserved amino acid motifs have been identified which suggest the presence of a hydroxo-bridged di-iron center in the active site of the alternative oxidase. On the basis of sequence comparison with other di-iron center proteins, a structural model for the active site of the alternative oxidase has been developed that has strong similarity to that of methane monoxygenase. Evidence is presented to suggest that the alternative oxidase of plant mitochondria is the newest member of the class II group of di-iron center proteins.

KEY WORDS: Alternative oxidase; sequence homology; hydroxo-bridged di-iron center proteins; mitochondria.

INTRODUCTION

The primary function of mitochondria is to synthesize ATP and provide carbon skeletons for biosynthetic purposes. In heterotrophic eukaryotic cells cytosolic ATP demands are met by the activity of the mitochondrial ATP synthase. In green plant cells, however, such demands can be met by photosynthetic photophosphorylation by indirect transfer of ATP from the chloroplast stroma to the cytosol (Moore *et al.*, 1992). An additional feature of plant mitochondrial metabolism relates to photorespiration which results in the formation of glycine, an important intermediate of this pathway (Oliver, 1995). Glycine is decarboxylated in the mitochondrial matrix via the combined action of glycine decarboxylase and serine hydroxy methyltransferase. Continued operation of the photorespiratory pathway requires regeneration of NAD^+, which can be achieved either by the respiratory chain or by transfer to the cytosol by metabolite shuttles (Wiskich and Meidan, 1992). An important question is therefore how plant mitochondria maintain an anaplerotic function under relatively high cytosolic ATP levels.

There is considerable evidence to suggest that the metabolic role of plant mitochondria is developmentally regulated because distinct biochemical and morphological changes have been demonstrated to occur in mitochondria as the plant cell matures and develops photosynthetically (Tobin and Rogers, 1992; Rhoads and McIntosh, 1992; Kearns *et al.*, 1992; Conley and Hanson, 1994; Lennon *et al.*, 1995). In tissues with a high metabolic rate, such as those involved in cell division and expansion, the production of ATP is a key metabolic role of mitochondria, but as the cell matures and becomes photosynthetically and photorespiratorily active, mitochondrial function changes to more of a biosynthetic role via the provision of carbon skeletons (Tobin and Rogers, 1992).

Plant mitochondria are well suited to both play a biosynthetic role and provide cytosolic ATP because, in addition to possessing Complexes I (NADH dehydrogenase), II (succinate dehydrogenase), III (bc_1 com-

[1] Department of Biochemistry, University of Sussex, Falmer, Brighton BN1 9QG, U.K.
[2] DCMB/Botany, Box 91000, Duke University, Durham, North Carolina 27708-1000.

0145-479X/95/0800-0367$07.50/0

plex) and IV (cytochrome *c* oxidase), most plant mitochondria also contain nonphosphorylating routes to molecular oxygen (Fig. 1). These include an externally located NAD(P)H dehydrogenase, an internal rotenone-insensitive NAD(P)H dehydrogenase that bypasses Complex I and, to varying degrees, a cyanide- and antimycin-insensitive alternative oxidase (Douce and Neuburger, 1989; Moore and Siedow, 1991). Thus, under low cytosolic ATP/ADP ratios (i.e., a low protonmotive force) plant mitochondria can synthesize ATP by oxidative phosphorylation, whereas under high ATP/ADP ratios (i.e., a high protonmotive force) respiratory activity can still occur either as a result of engagement of these nonphosphorylating pathways or as a consequence of non-ohmicity, which acts either through increased proton conductance of the inner membrane (i.e., engagement of a leak pathway) or as a result of redox slippage (Moore *et al.*, 1994; Whitehouse and Moore, 1995).

PROPERTIES OF THE ALTERNATIVE OXIDASE

Cyanide- and antimycin-resistant respiratory activity is widespread among the plant kingdom and its capacity can vary from as little as a few percent of total oxygen consumption as in the case of freshly isolated potato tuber mitochondria to as much as 100% in the case of mitochondria isolated from thermogenic spadices of *Arum maculatum* or *Sauromatum guttatum.* It can be induced, in some plants, by factors such as (1) wounding, (2) low, nonfreezing temperatures, (3) salicylic acid, (4) changes in carbon status, and (5) in plant tissue cultures, yeast, and fungi, inhibition of the main respiratory pathway (Moore and Siedow, 1991; McIntosh, 1994).

The alternative pathway of plant mitochondria branches from the main mitochondrial respiratory chain at the level of the ubiquinone pool and is nonprotonmotive. The alternative oxidase protein is an integral membrane protein with its active site located on the matrix side of the inner membrane (Moore and Siedow, 1991). The enzyme catalyzes the oxidation of ubiquinol to ubiquinone and the reduction of O_2 to H_2O and is inhibited by primary hydroxamic acids such as salicylhydroxamic acid (Siedow and Berthold, 1986; Moore and Siedow, 1991). A key characteristic of the alternative oxidase is the lack of any unique electron paramagnetic resonances in either membrane bound (Rich *et al.*, 1977; Moore and Siedow, 1991) or partially purified preparations. The latter preparations also display no optical absorbance above 350 nm (Berthold and Siedow, 1993).

Extensive kinetic investigations (Moore *et al.*, 1988; Dry *et al.*, 1989: Moore and Siedow, 1991; Day

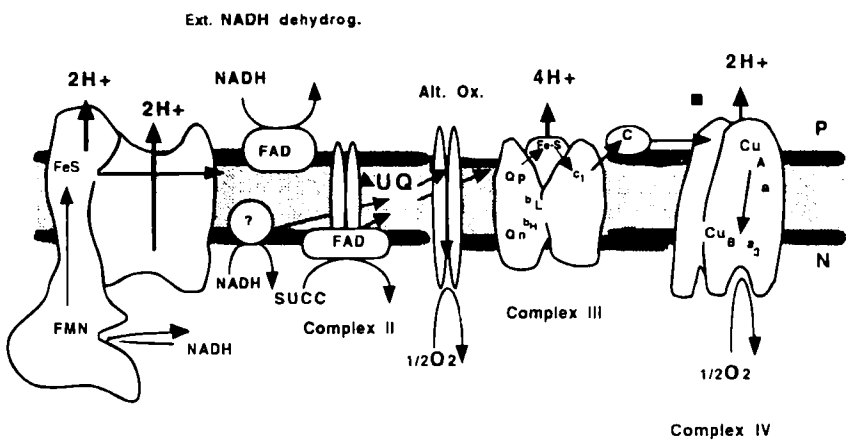

Fig. 1. Diagrammatic representation of the plant mitochondrial respiratory chain. Abbreviations used: NADH, nicotinamide adenine dinucleotide-reduced; FMN, flavin mononucleotide; FAD, flavin adenine dinucleotide; FeS, iron-sulfur center, b_L and b_H, cytochromes *b*, low and high potential, respectively; *c* and *c*1, cytochromes *c* and c_{21}; *a* and a_{21}, cytochromes *a* and a_{21}; UQ, ubiquinone pool; P and N refer to the cytoplasmic and matrix facing sides of the inner membrane; Q_p and Q_n refer to ubiquinone binding sites close to the P and N face of the membrane; the question mark signifies a dehydrogenase yet to be established.

et al., 1991; Moore *et al.*, 1992; Moore and Siedow, 1992; Siedow and Moore, 1993) have revealed that engagement of the alternative pathway is governed by the redox state of the Q-pool such that electron flow through the pathway only occurs when the reduction state of the pool exceeds a certain threshold value. Beyond this threshold, engagement increases as a nonlinear function of the Q-pool reduction state. A two-step reduction model has been developed, the steady-state rate equation of which has been used to accurately simulate data describing the relationship between Q-pool redox poise and alternative oxidase activity (Siedow and Moore, 1993). The model suggests that the reduction of oxygen by the alternative oxidase proceeds via the initial formation of a four-electron reduced enzyme (Siedow and Moore, 1993). Recently, the two-step reduction model has been modified to incorporate an activation step of the fully reduced enzyme before it reacts with oxygen (Ribas-Carbo *et al.*, 1994). This additional step was introduced to accommodate the finding that the affinity of the alternative oxidase for oxygen decreases with increased reduction of the ubiquinone pool.

Although there have been attempts to isolate the alternative oxidase from a variety of plant sources (Moore and Siedow, 1991), characterization of the metal cofactors associated with the alternative oxidase active site has been hindered by the lack of a purified fraction. Metal analyses of partially purified alternative oxidase preparations have been inconclusive; Fe, Cu, and Mn have each been reported in varying amounts (Huq and Palmer, 1978; Palmer and Huq, 1981; Bonner *et al.*, 1986). The observation that the primary product of oxygen reduction is water, and not peroxide, suggests that the alternative oxidase active site contains a coupled transition metal center (Naqui and Chance, 1986). The strongest evidence that iron is associated with the alternative oxidase active site was obtained by Minagawa *et al.* (1990) who found that growth of *H. anomala* in the presence of antimycin and the Fe(II) chelator *o*-phenanthroline, although resulting in the synthesis of the 36-kDa alternative oxidase protein, was not associated with any measurable alternative pathway activity. The subsequent addition of Fe(II) to the cells, however, did result in the rapid appearance of alternative pathway activity.

cDNA clones encoding the alternative oxidase protein have been reported from several plant species, including *Sauromatum guttatum, Arabidopsis,* soybean, mango, and tobacco (Rhoads and McIntosh, 1991; Kumar and Soll, 1992; Whelan *et al.*, 1993; Vanlerberghe and McIntosh, 1994), as well as the yeast *Hansenula anomala* (Sakajo *et al.*, 1991). Secondary structure predictions of the mature form of the alternative oxidase protein reveals three regions expected to be strongly α-helical. Hydropathy analysis suggests that within two of these regions are spans of relatively high hydrophobicity which are likely to produce membrane-spanning helices (Moore and Siedow, 1991; Rhoads and McIntosh, 1991; Sakajo *et al.*, 1991; McIntosh, 1994). The remainder of the protein is quite hydrophilic, with charged residues distributed over much of its mass. Proteolysis studies suggest that both the C- and N-termini are located on the matrix face of the membrane (Siedow *et al.*, 1992). A model for the structure of the alternative oxidase protein is presented in Fig. 2 in which the two large hydrophilic domains, on either side of the two membrane-anchoring helices (Moore and Siedow, 1991), are both located on the matrix side of the inner mitochondrial membrane (Rasmusson *et al.*, 1990; Siedow *et al.*, 1992). Until very recently (Siedow *et al.*, 1995) the deduced amino acid sequences did not shed much light on the nature of the active site, since no major sequence similarities with other proteins were identified (Moore and Siedow, 1991; McIntosh, 1994).

Another structural feature of the alternative oxidase was revealed with the demonstration that the protein exists as a dimer in the inner mitochondrial membrane, based upon results using chemical cross-linking reagents (Umbach and Siedow, 1993). Further, the dimeric alternative oxidase exists in one of two states, an oxidized state, in which the dimer is covalently cross-linked by an intermolecular disulfide bridge and a reduced state, in which the disulfide bond is reduced to its component sulfhydryls (Fig. 2) and the dimeric structure is maintained through noncovalent interactions (Umbach and Siedow, 1993). The activity of the alternative oxidase is dependent upon the redox state of this sulfhydryl/disulfide system, with the reduced form being four- to fivefold more active than the oxidized form (Umbach and Siedow, 1993; Umbach *et al.*, 1994).

DI-IRON PROTEINS

Some physical properties of the partially purified alternative oxidase (Berthold and Siedow, 1993), such as the lack of any standard EPR signals or any absorbance above 350 nm in the oxidized and fully reduced forms, are unusual for a metalloprotein. How-

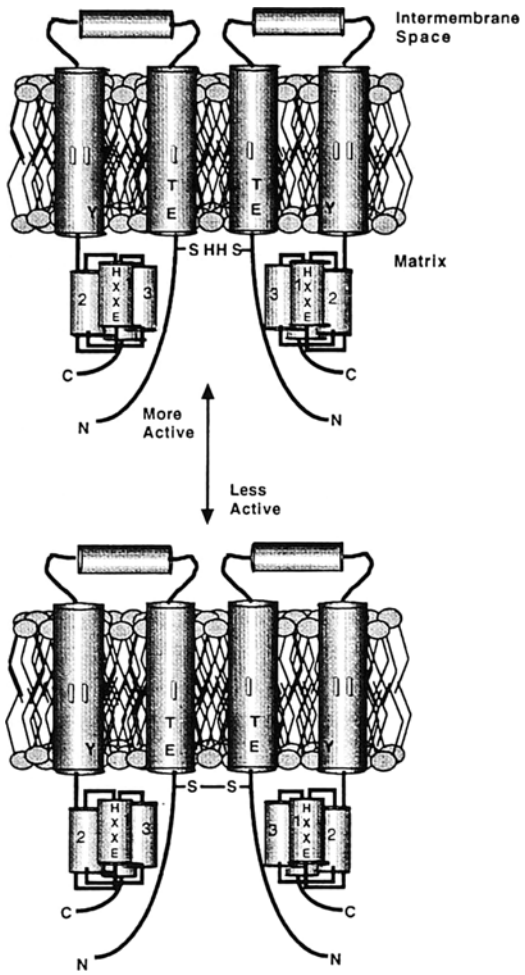

Fig. 2. Structural model of the dimeric alternative oxidase. The proposed structure of the alternative oxidase protein shows the postulated two transmembrane helices and the four-helix bundle (containing the coupled binuclear iron center) which is located in the carboxy-terminal hydrophilic domain of the protein. The highly conserved amino acid residues Glu, Thr, and Tyr, located in the two transmembrane helices, are proposed to be involved in the postulated quinone binding site. In the oxidized state the dimer is covalently linked while in its reduced state (which is 4–5-fold more active) the dimeric structure is probably maintained through noncovalent interactions. For further details see text.

ever, they are reminiscent of the properties of methane monooxygenase (MMO) (Vincent *et al.*, 1990; Wilkins, 1992; Lipscombe, 1994) and led us to ascertain whether there are any amino acid sequence similarities between these two proteins (Moore *et al.*, 1995; Siedow *et al.*, 1995).

MMO belongs to a class of metalloproteins, which also includes hemerythrin (Hr), the R2 subunit of ribonucleotide reductase (R2), and soluble fatty acid desaturases, which are characterized by the possession of oxo- or hydroxo-bridged di-iron centers (Sanders-Loehr *et al.*, 1989; Wilkins and Dalton, 1994; Fox *et al.*, 1994). Such centers contain two iron atoms connected to each other either by a μ-oxo- or μ-hydroxo-bridging ligand. In addition to containing an oxo- or hydroxo-bridging ligand, at least one other bridging ligand is a carboxylate group, with the remaining iron ligands being N atoms from histidines and O atoms from Glu or Asp residues. In general, proteins belonging to this group are water soluble, and physical characterizations suggest that the binuclear iron sites can exist in three oxidation states. The oxidized form contains two antiferromagnetically coupled high-spin Fe(III) atoms (Vincent *et al.*, 1990: Wilkins 1992) while the mixed valent Fe(II)–Fe(III) species exhibit EPR signals of $g = < 2$, indicative of a non-heme bridged di-iron center. In the fully reduced state, both iron atoms are Fe(II) and remain ferromagnetically coupled (Wilkins, 1992). These binuclear iron proteins show no standard EPR signal in either the oxidized or fully reduced states. However, fully reduced [Fe(II)Fe(II)] MMO does display an integer spin EPR signal at $g = 16$ (Fox *et al.*, 1988; Hendrich *et al.*, 1990). MMO is unique among the binuclear iron proteins in having no absorbance above 350 nm, a consequence of possessing a μ-hydroxo-bridged ligand instead of the μ-oxo-bridged system found in ribonucleotide reductase and hemerythrin (Turowski *et al.*, 1994).

The X-ray crystal structures for Hr, R2, and MMO have all been solved and in all cases the di-iron centers are buried in four α-helices arranged in the form of a four-helix bundle that acts as a scaffold to bind the iron atoms (Holmes *et al.*, 1991; Nordlund and Eklund, 1993; Rosenzweig *et al.*, 1993). Analysis of differences in the primary sequence motifs in the four-helix bundle and structural properties revealed by X-ray crystallography, have led to the di-iron proteins being grouped into three classes, I, II, and III (Fox *et al.*, 1994; Shanklin *et al.*, 1994). This classification is based upon the nature of the ligands to the iron atom and the alignment of the Fe–Fe axis relative to that of the major axis of the four-helical bundle.

An example of the class I type of di-iron protein is Hr, X-ray crystal data of which suggest that the two iron atoms are oriented perpendicular to a contiguous four-helix bundle, with the majority of the ligands being provided by N atoms from five His residues and the remaining ligands being due to bridging carboxylates and the oxo-bridge (Holmes *et al.*, 1991).

Members of the class II type of di-iron proteins include the R2 protein of ribonucleotide reductase, the hydroxylase component of MMO, and the stearoyl-acyl carrier protein Δ^9 desaturase (Wilkins and Dalton, 1994; Fox *et al.*, 1994; Shanklin *et al.*, 1994). X-ray crystallography of the R2 protein (Nordlund and Eklund, 1993) and MMO (Rosenzweig *et al.*, 1993) indicate that, in contrast to Hr, the iron atoms in the active site of these enzymes are oriented parallel to the four-helical bundle, the helices of which are arranged in a noncontiguous fashion. Of particular importance is the finding that all proteins within class II are characterized by two copies of the primary sequence motif (D/E-X-X-H) that are buried in two of the four helices of the bundle (Nordlund *et al.*, 1992). Both of the histidines and one of the two carboxylates serve as monodentate ligands to the iron atoms in the binuclear cluster, while the second carboxylate acts as a bidentate ligand, bridging the two iron atoms. The remaining protein ligands to the iron atoms are provided by carboxylate residues, one in each of the other two helices of the four-helical bundle. Additional features of the class II di-iron proteins include the presence of a hydrophobic cavity formed adjacent to the iron center by a series of conserved residues within the four-helical bundle and the presence of conserved residues that participate in a hydrogen bonding network.

An additional class of di-iron proteins (class III) has been characterized recently which includes the membrane-associated desaturases, alkane hydroxylase, and xylene monooxygenase (Shanklin *et al.*, 1994). In this class of proteins eight conserved His residues have been suggested to be essential for catalytic function, probably by acting as ligands for the two iron atoms contained in these enzymes.

A MODEL OF THE ACTIVE SITE OF THE ALTERNATIVE OXIDASE

Analysis of the plant alternative oxidase amino acid sequences reveals the presence of several highly conserved regions located in the carboxy-terminal hydrophilic domain of the protein (Fig. 3; Glu-268 to Glu-324 in *S. guttatum*), beginning just beyond the second membrane-spanning region. The motifs, Glu-Glu-A-I-His (helix 1), and Asp-Glu-A-H-His (helix 4), are found in two of these regions. They correspond to the motifs involved in ligating the binuclear iron cluster of MMO (Rosenzweig *et al.*, 1993), with the single conservative substitution of a glutamate for an aspartate residue next to the liganding glutamate in the more N-terminal of the two sequences (Fig. 2 of Siedow *et al.*, 1995). Other highly conserved residues worthy of note include an Asp-283 (helix 2), Ile-295, and Tyr-299 (helix 3) and Val-315 (helix 4)(Fig. 3).

Using these putative iron-binding motifs in the alternative oxidase sequence, a model of a four-helix bundle was developed in an attempt to identify the nature of the active site of this enzyme (Siedow *et al.*, 1995). In the R2 protein and MMO (Nordlund *et al.*, 1990; Rosenzweig *et al.*, 1993), the four-helical bundle that forms the metal binding site contains 30–35 residues per helical region (Sheriff *et al.*, 1987; Nordlund *et al.*, 1990; Rosenzweig *et al.*, 1993), with two of the four helices (helices C and F) each containing one of the two Glu-X-X-His motifs. In the alternative oxidase, the total span from the first to the second Glu-X-X-His motif is just under 60 residues, considerably shorter than that observed in R2 and MMO, necessitating shorter helical spans. In this model, the two Glu-X-X-His iron-binding motifs are located on helices 1 and 4, which are oriented antiparallel (Fig. 4), analogous to helices C and F in MMO (see Fig. 2 of Siedow *et al.*, 1995). It can be seen from Fig. 3 that in this model helix 2 contains a conserved aspartate residue (Asp-283), located toward the amino terminus, which may act as a ligand to iron atom Fe I (analogous to Glu-114 in helix B of MMO; Rosenzweig *et al.*, 1993). Helix 3 appears to lack any highly conserved glutamate or aspartate residues, in contrast to that observed in R2 and MMO but analogous to the soluble fatty acyl desaturases (Fox *et al.*, 1994). In the R2 protein of *E. coli* ribonucleotide reductase, Asp-84 in helix B, the analogue to Glu-114 in MMO, acts as a bidentate ligand to Fe1 (Nordlund *et al.*, 1990). If Glu-319 in helix 4 were to act as a bidentate ligand to iron atom Fe2 in the alternative oxidase active site in a fashion analogous to that of Asp-84 binding to Fe1 in ribonucleotide reductase, the need for the additional carboxylate ligand in helix 3 would be eliminated.

The four-helical bundle shown in Fig. 4 requires tight turns containing three residues each at the helices 1/2 and 2/3 junctions. Analogous tight turns have been found previously in proteins having a four helix-bundle motif (Lederer *et al.*, 1981; Sheriff *et al.*, 1987). The alignment of the two Glu-X-X-His iron-binding motifs on helices 1 and 4 can be arranged exactly as found in MMO helices C and F, respectively (Rosenzweig *et al.*, 1993), suggesting that the di-iron axis is oriented parallel to the long axis of the four-helix bundle. How-

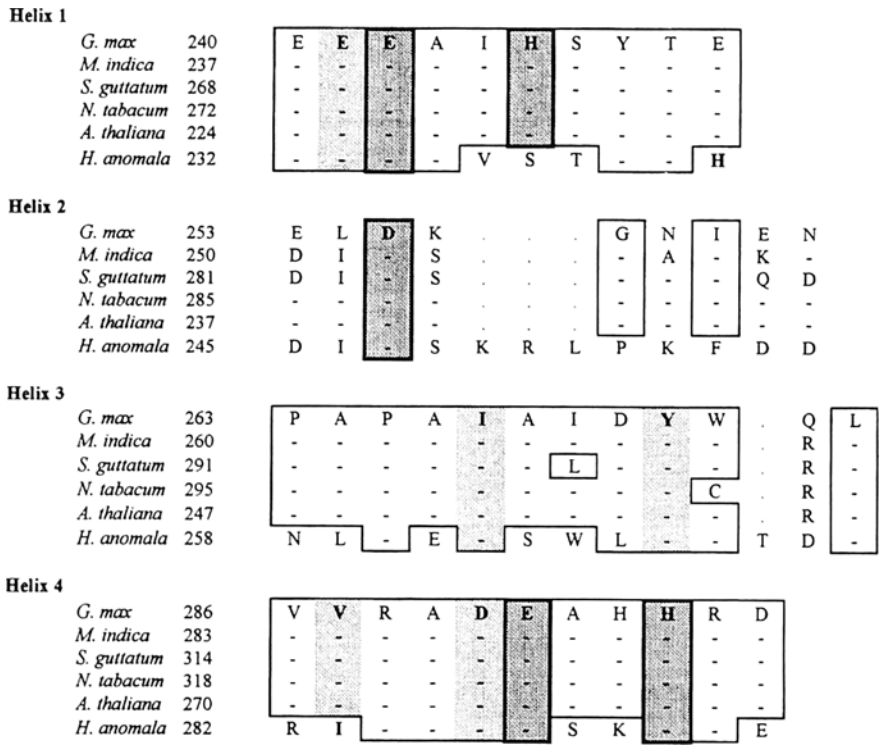

Fig. 3. Comparison of the alternative oxidase deduced amino acid sequences within the region of the proposed binuclear iron center. All alternative oxidase sequences are aligned relative to the conserved glutamate residue (Glu-270) of *S. guttatum*. The sequences represented are for the unprocessed alternative oxidase proteins from soybean (*G. max*), mango (*M. indica*), *Arabidopsis* (*A. thaliana*), tobacco (*N. tabacum*), *Sauromatum guttatum* (*S. guttatum*) and *Hansenula anomala* (*H. anomala*). Bold and heavily shaded residues represent amino acids that are involved directly in the formation of the coupled binuclear iron center, as outlined in the text. Dashes (—) denote residues identical to those found in the soybean sequence, and dots (·) are used to indicate breaks in the plant amino acid sequences needed to maximize the alignment of conserved residues in the *H. anomala* sequence.

ever, the arrangement of the bundle does differ from that of other Class II type oxo-bridged proteins by the fact that in the alternative oxidase the ligands arise from four contiguous helices (similar to that observed in Class I proteins).

Using the highly conserved residues located in the carboxy-terminal hydrophilic domain of the alternative oxidase, a hypothetical structure of a binuclear iron center in the protein is proposed which is comparable to that seen with the R2 protein and MMO active sites (Fig. 5). In this structure, the ferric center is coordinated by two histidines, two glutamates (one of which is bridging), one aspartate, and two water molecules. Finally, a bridging hydroxo atom is incorporated into the alternative oxidase active site model (Fig. 5C) to account for the lack of absorbance above 350 nm, analogous to MMO (Vincent *et al.*, 1990; Wilkins, 1992). Similar to other class II di-iron pro-

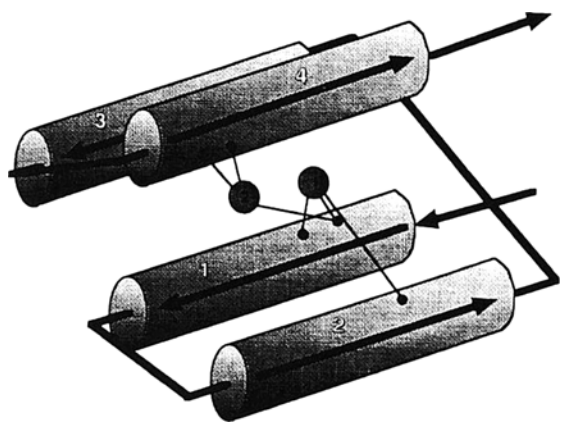

Fig. 4. Diagrammatic representation of the orientation of the binuclear iron center relative to the major axis of the four-helical bundle that provides the iron coordinating ligands in the proposed active site of the alternative oxidase. In this model, the two Glu-X-X-His iron-binding motifs are located on helices 1 and 4, which are orientated in an antiparallel fashion.

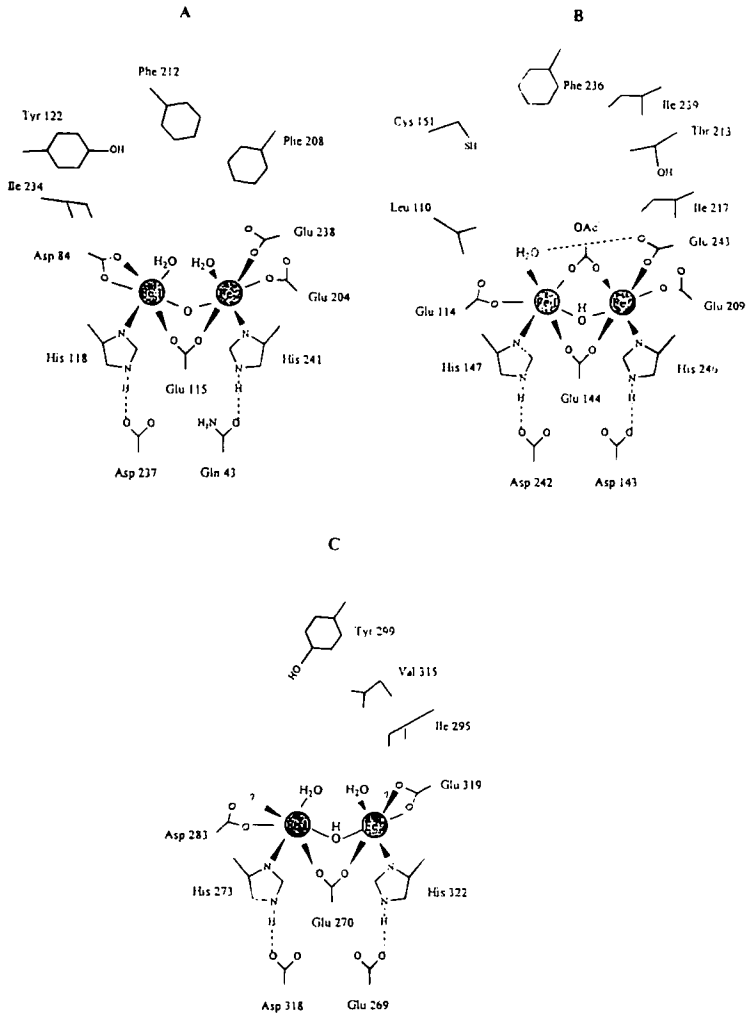

Fig. 5. Diagrammatic representation of the liganding pattern for the coupled binuclear iron center of (A) the R2 component of *E. coli* ribonucleotide reductase, (B) the *Methylococcus capsulatus* methane monooxygenase, and (C) the proposed di-iron center of the alternative oxidase. The residue numbers refer to the amino acid sequence for the unprocessed polypeptide from *S. guttatum*. For further details see text.

teins, a conserved carboxylate residue is found adjacent to each Glu-X-X-His sequence which is positioned to the hydrogen bond to the liganding histidine of the alternate Glu-X-X-His (Figs. 5A and B). The similarity of the proposed active site of the alternative oxidase to the active sites of MMO and the R2 protein of ribonucleotide reductase is striking.

The similarity in structures even extends to the hydrophobic pocket. For instance, Val-315 is in a position analogous to that of Ile-239 in MMO (Fig. 5), suggesting that it may be a likely candidate to line the hydrophobic pocket in the active site (Rosenzweig *et al.*, 1993). This position is conserved as either an isoleucine or a valine among all MMOs, R2 proteins, and the soluble fatty acyl desaturases (Nordlund *et al.*, 1992; Fox *et al.*, 1994). In the proposed alternative oxidase active site, the conserved residue, Tyr-299, can also be aligned within the hydrophobic pocket in the position occupied by Ile-217 and Phe-212 in helix E of MMO and the R2 protein of ribonucleotide reductase, respectively (Fig. 5). In the R2 protein, Phe-212 combines with Phe-208 (equivalent to Thr-213 in MMO) to line the hydrophobic pocket. In the alternative oxidase, Ile-295 occupies the position analogous to Phe-208 in the R2 protein and is conserved among all alternative oxidase sequences. To summarize, using

conserved residues within the plant alternative oxidase amino acid sequence, a structural model incorporating a hydroxo-bridged binuclear iron center and a hydrophobic pocket held within a four-helix bundle, analogous to the iron center in MMO, can readily be developed (Fig. 5C). The proposed structure for the primary ligation sphere of the di-iron center in the alternative oxidase suggests that it is intermediate to both MMO and the R2 protein. As with the R2 protein and probably MMO, there are only two bridging groups, an oxo- and a glutamate residue between the two iron atoms. The remaining ligands are a histidine, probably a bidentate aspartate, and water coordinated to Fe1, and a histidine, a bidentate glutamate, and water to Fe2.

For such a model to be tenable it is important that it can also account for the alternative oxidase in other systems such as *H. anomala*. Analysis of the primary amino acid sequence of the alternative oxidase in this organism (Fig. 3) also reveals a high degree of residue conservation particularly in the proposed ligation sphere of the di-iron cluster. While helices 3 and 4 and Asp-247 (the analogue of Asp-283) closely match that found in the plant oxidase, it should be noted from Fig. 2 that the conserved histidine in helix 1 has been replaced by serine. Although there is evidence in the literature to suggest that serine can ligate to iron-sulfur clusters (Fujinaga *et al.*, 1993), it would be surprising if substitution of a His for a Ser residue did not result in modification of the physical properties of the *Hansenula* enzyme. Whether this is indeed the case will have to await further detailed analysis of properties of this particular enzyme. Should serine prove not to be a suitable ligating amino acid, other possibilities, such as His-241, will need to be considered (Siedow *et al.*, 1995).

Quinone-Binding Site

An additional structural feature that must exist within the active site of the alternative oxidase is a binding site for ubiquinol, the reducing substrate of the oxidase. X-ray structures of the photosynthetic reaction centers from *Rhodopseudomonas viridis* and *Rhodobacter sphaeroides* have provided the first detailed picture of quinone binding sites within an integral membrane protein (Deisenhofer *et al.*, 1985; Allen *et al.*, 1988). The Q_A and Q_B binding sites each consist of a pocket lined by residues contributed from the ends of two adjacent membrane-spanning helices plus the interhelical loop region that is also helical and appears to shield the quinone binding pocket from the aqueous environment (Allen *et al.*, 1988; Michel *et al.*, 1986; Sinning *et al.*, 1990). For each quinone binding site, the two membrane-spanning helices appear to form a hydrophobic binding region, while specific quinone head group–protein interactions involve primarily residues in the interhelical region (Allen *et al.*, 1988; Michel *et al.*, 1986). In the tight-binding Q_A site, these interactions include ring overlap with a tryptophan and hydrogen bonding to a histidine residue and a peptide nitrogen. In the more weakly bound Q_B site, quinone head group interactions involve hydrogen bonding with serine and histidine residues, and a peptide nitrogen (Allen *et al.*, 1988; Sinning *et al.*, 1990).

More recently, attempts have been made to map the quinol oxidation site (Qp) in complex III of the mitochondrial electron transfer chain (Link *et al.*, 1993). During the oxidation of ubiquinol at the Qp site, one electron is transferred to the Rieske iron-sulfur center while a second electron is donated to the low-potential heme on cytochrome *b* (Trumpower, 1990). Mapping this quinol binding site relied heavily on the generation of mutations of cytochrome *b* in yeast (di Rago *et al.*, 1989; Tron *et al.*, 1991; Geier *et al.*, 1992), mouse culture cells (Howell, 1990), and *Rhodobacter capsulatus* (Robertson *et al.*, 1990) selected for respiratory (yeast, mouse) or photosynthetic (*Rhodobacter*) growth in the presence of Qp site inhibitors. The residues in cytochrome *b* that can be changed to give an inhibitor-resistant phenotype are limited in number and cluster in areas that include two membrane-spanning regions and two interhelical regions. The model of the quinol oxidation site that results from this work is analogous to the quinone sites in the photosynthetic reaction centers (Link *et al.*, 1993). The quinone binding pocket is formed by the ends of two transmembrane helices plus a set of residues contributed by two interhelical regions that cap the site and probably provide ligands to the quinol head group. Inhibitor-resistant mutations have also been mapped for the antimycin-sensitive quinone reduction site (Qn) in complex III located toward the matrix side of the inner mitochondrial membrane in yeast (di Rago and Colson, 1988; di Rago *et al.*, 1990), but no attempt to develop a similar binding site model has been published.

Like complex III, the alternative oxidase must contain a ubiquinol oxidation site. The most highly conserved amino acid sequences of the alternative oxi-

dase protein are located within the two postulated membrane-spanning helices and the hydrophilic region on the C-terminal side of the second membrane-spanning helix (McIntosh, 1994; Siedow *et al.*, 1995). It is conceivable that the matrix-oriented half of the two membrane helices forms the scaffolding for a ubiquinol binding pocket, in conjunction with the adjacent carboxy-terminal hydrophilic region just outside the membrane (Fig. 2). Interestingly, in the first membrane-spanning helical region, among the 11 residues that are conserved in all known sequences, eight are in the N-terminal half of the helix that is oriented toward the matrix side of the membrane. This model of the quinol oxidation site of the alternative oxidase complements the model described above for the catalytic binuclear iron center. The four-helical bundle containing the iron center is located in the carboxy-terminal stretch of amino acids just past the domain that makes up the quinol oxidation site. In this model, the binuclear iron center should be well positioned to undergo facile reduction by ubiquinol present in the postulated quinol-binding site. This model is obviously speculative, but it provides a framework for subsequent studies that may give insight into residues that are associated with the quinol oxidation site.

Mechanism of Oxygen Reduction

Steady-state kinetic analysis suggests that the oxidase reacts with two molecules of reduced ubiquinone before binding and subsequently reducing oxygen to water (Siedow and Moore, 1993; Ribas-Carbo *et al.*, 1994). Obviously the presence of a single binuclear iron center (a two-electron carrier) in the active site of the alternative oxidase is insufficient to account for such a mechanism. The two sets of di-iron sites in the alternative oxidase dimer could act in a cooperative manner to generate the functional oxygen-reducing species. However, the observation from radiation inactivation analysis that the functional molecular mass of the alternative oxidase is equivalent to that of the monomer would appear to preclude this (Berthold *et al.*, 1988). The presence of additional centers and the involvement of ferryl complexes could each account for the formation of a four-electron reduced oxidase. There is at present, however, no spectroscopic evidence in favor of an additional center. Ferryl complexes have been proposed as active intermediates during substrate oxidation by MMO (Dalton *et al.*, 1993), although direct evidence for their involvement in the catalytic cycle of MMO is debatable (Shteinman, 1995). An additional possibility for the alternative oxidase is that the four-electron reduced oxidase suggested by the steady-state kinetic data actually represents the two-electron reduced enzyme plus a bound molecule of reduced ubiquinone (Siedow *et al.*, 1995). Clearly, additional studies are needed to ascertain whether such a mechanism can fully account for the catalytic activity of the alternative oxidase.

Future Developments

The development of a structural model for the active site of the alternative oxidase opens up exciting possibilities for future investigations. One possibility, currently being pursued by our laboratories, is the expression of the plant enzyme in *Schizosaccharomyces pombe* and *Escherichia coli* in attempts to probe structure–function relationships using site-directed mutagenesis. Such an approach would confirm whether the conserved motifs and residues are essential for catalytic activity of the oxidase. Other possibilities include the functional overexpression of the oxidase to produce sufficient protein to facilitate physical analysis of the enzyme using EPR and ENDOR techniques. Such techniques would provide valuable information on the electronic and geometrical structures of the iron center. Additionally, investigations are currently under way to design and synthesize a maquette of the active site of the alternative oxidase in a manner so successfully pursued by the Dutton laboratory for multiheme proteins (Robertson *et al.*, 1994). It is hoped that such an approach will establish the minimal requirements for the function of the natural counterpart and perhaps reveal why members of the di-iron group of proteins, of which the alternative oxidase is the newest member, are so diverse in function. Further advances in our understanding of the alternative oxidase will be achieved when the physical properties of the purified protein become known, but it is hoped that progress made to date will serve as a catalyst for the challenging and important work yet to be done.

ACKNOWLEDGMENTS

This work was supported by grants from the Biotechnology and Biological Science Research Council to A.L.M and from the National Science Foundation (MCB-9407759) to J.N.S.

REFERENCES

Allen, J. P., Feher, G., Yeates, T. O., Komiya, H., and Rees, D. C. (1988). *Proc. Natl. Acad. Sci. USA* **85**, 8487–8491.

Berthold, D. A., and Siedow, J. N. (1993). *Plant Physiol.* **101**, 113–119.

Berthold, D. A., Fluke, D. J., and Siedow, J. N. (1988). *Biochem. J.* **252**, 73–77.

Bonner, W. D., Clarke, S. D., and Rich, P. R. (1986). *Plant Physiol.* **80**, 838–842.

Conley, C. A., and Hanson, M. R. (1994). *The Plant Cell* **6**, 85–91.

Dalton, H., Wilkins, P. C., and Jiang, Y. (1993). *Biochem. Soc. Trans.* **21**, 749–752.

Day, D. A., Dry, I B., Soole, K. L., Wiskich, J. T., and Moore, A. L. (1991). *Plant Physiol.* **95**, 948–953.

Deisenhofer, J., Epp, O., Miki, K., Huber, R., and Michel H. (1985). *Nature* **318**, 618–624.

di Rago, J.-P., and Colson, A.-M. (1988). *J. Biol. Chem.* **263**, 12564–12570.

di Rago, J.-P., Coppee, J.-Y., and Colson, A.-M. (1989). *J. Biol. Chem.* **264**, 14543–14548.

di Rago, J.-P., Perea, J., and Colson, A.-M. (1990). *FEBS Lett.* **263**, 93–98.

Douce, R., and Neuburger, M. (1989). *Annu. Rev. Plant Physiol. Plant Mol. Biol.* **40**, 371–414.

Dry, I. B., Moore, A. L., Day, D. A., and Wiskich, J. T. (1989). *Arch. Biochem. Biophys.* **273**, 148–157.

Fox, B. G., Surerus, K. K., Munck, E., and Lipscomb, J. D. (1988). *J. Biol. Chem.* **263**, 10553–10556.

Fox, B. G., Shanklin, J., Somerville, C., and Munck, E. (1993). *Proc. Natl. Acad. Sci. USA* **90**, 2486–2490.

Fox, B. G., Shanklin, J., Ai, J., Loehr, T. M., and Sanders-Loehr, J. (1994). *Biochemistry* **33**, 12776–12786.

Fujinaga, J., Gaillard, J., and Meyer, J. (1993). *Biochem. Biophys. Res. Commun.* **194**, 104–111.

Geier, B. M., Schagger, H., Brandt, U., and von Jagow, G. (1992). *Eur. J. Biochem.* **208**, 375–380.

Hendrich, M. P., Munck, E., Fox, B. G., and Lipscomb, J. D. (1990). *J. Am. Chem. Soc.* **112**, 5861–5865.

Holmes, M. A., Le Trong, I., Turley, S., Sieker, L. C., and Stenkamp, R. E. (1991). *J. Mol. Biol.* **218**, 583.

Howell, N. (1990). *Biochemistry* **29**, 8970–8977.

Huq, S., and Palmer, J. M. (1978). *FEBS Lett.* **95**, 217–220.

Kearns, A., Whelan, J., Young, S., Elthon, T. E., and Day, D. A. (1992). *Plant Physiol.* **99**, 712–717.

Kumar, A. M., and Soll, D. (1992). *Proc. Natl. Acad. Sci. USA* **89**, 10842–10846.

Lederer, F., Glatigny, A., Bethge, P. H., Bellamy, H. D., and Mathews, F. S. (1981). *J. Mol. Biol.* **148**, 427–448.

Lennon, A. M., Pratt, J., Leach, G., and Moore, A. L. (1995). *Plant Physiol.* **107**, 925–932.

Link, T. A., Haase, U., Brandt, U., and von Jagow, G. (1993). *J. Bioenerg. Biomembr.* **25**, 221–232.

Lipscombe, J. D. (1994). *Annu. Rev. Microbiol.* **48**, 371–399.

McIntosh, L. (1994). *Plant Physiol.* **105**, 781–786.

Michel, H., Epp, O., and Deisenhofer, J. (1986). *EMBO J.* **5**, 2445–2451.

Minagawa, N., Sakajo, S., Komiyama, T., and Yoshimoto, A. (1990). *FEBS Lett.* **267**, 114–116.

Moore, A. L., and Siedow, J. N. (1991). *Biochim. Biophys. Acta* **1059**, 121–140.

Moore, A. L., Dry, I. B., and Wiskich, J. T. (1988). *FEBS Lett.* **235**, 76–80.

Moore, A. L., Siedow, J. N., Fricaud, A-C., Vojnikov, V., Walters, A. J., and Whitehouse, D. G. (1992). In *Plant Organelles* (Tobin, A. K., ed.), Society for Experimental Biology Seminar Series, Vol. 50, Cambridge University Press, Cambridge, pp. 188–210.

Moore, A. L., Leach, G. L., Whitehouse, D. G., van den Bergen, C. W. M., Wagner, A. M., and Krab, K. (1994). *Biochim. Biophys. Acta* **1187**, 145–151.

Moore, A. L., Umbach, A. L., and Siedow, J. N. (1995). *Biochem. Soc. Trans.* **23**, S 151.

Naqui, A., and Chance, B. (1986). *Annu. Rev. Biochem.* **55**, 137–166.

Nordlund, P., and Eklund, H. (1993). *J. Mol. Biol.* **232**, 123.

Nordlund, P., Sjoberg, B.-M., and Eklund, H. (1990). *Nature (London)* **345**, 593–598.

Nordlund, P., Dalton, H., and Eklund, H. (1992). *FEBS Lett.* **307**, 257–262.

Oliver, D. G. (1994). *Annu. Rev. Plant Physiol. Plant Mol. Biol.* **45**, 323–337.

Palmer, J. M., and Huq, S. (1981). In *Cyanide in Biology* (Vennesland, B., Conn, E. E., Knowles, C. J., Westley, J., and Wissing, F. eds), Academic Press, New York, pp. 451–460.

Rasmusson, A. G., Moller, I. M., and Palmer, J. M. (1990). *FEBS Lett.* **259**, 311–314.

Rhoads, D. M., and McIntosh, L. (1991). *Proc. Natl. Acad. Sci USA* **88**, 2122–2126.

Rhoads, D. M., and McIntosh, L. (1992). *The Plant Cell* **4**, 1131–1139.

Ribas-Carbo, M., Wiskich, J. T., Berry, J. A., and Siedow, J. N. (1994). *Biochim. Biophys. Acta* **1188**, 205–212.

Rich, P. R., Moore, A. L., Ingledew, W. J., and Bonner, W. D. (1977). *Biochim. Biophys. Acta* **462**, 501–514.

Robertson, D. E., Daldal, F., and Dutton, P. L. (1990). *Biochemistry* **29**, 11249–11260.

Robertson, D. E., Farid, R. S., Moser, C. C., Urbauer, J. L., Mulholland, S. E., Pidikiti, R., Lear, J. D., Wand, A. J., DeGrado, W. F., and Dutton, P. L. (1994). *Nature (London)* **368**, 425–432.

Rosenzweig, A. C., Frederick, C. A., Lippard, S. J., and Nordlund, P. (1993). *Nature* **366**, 537543.

Sanders-Loehr, J., Wheeler, W. D., Shiemke, A. K., Averill, B. A., and Loehr, T. M. (1989). *J. Am. Chem. Soc.* **111**, 8084–8093.

Shanklin, J., Whittle, E., and Fox, B. G. (1994). *Biochemistry* **33**, 12787–12794.

Sheriff, S., Hendrickson, W. A., and Smith, J. L. (1987). *J. Mol. Biol.* **197**, 273–296.

Shteinman, A. A. (1995). *FEBS Lett.* **362**, 5–9.

Siedow, J. N., and Berthold, D. A. (1986). *Physiol. Plant.* **66**, 569–573.

Siedow, J. N., and Moore, A. L. (1993). *Biochim. Biophys. Acta* **1142**, 165–174.

Siedow, J. N., Whelan, J., Kearns, A., Wiskich, J. T., and Day, D. A. (1992). In *Molecular, Biochemical and Physiological Aspects of Plant Respiration* (Lambers, H., and van der Plas, L. H. W., eds.), SPB Academic Publishing, The Hague, pp. 19–27.

Siedow, J. N., Umbach, A. L., and Moore, A. L. (1995). *FEBS Lett.* **362**, 10–14.

Sinning, I., Koepke, J., Schiller, B., and Michel, H. (1990). *Z. Naturforsch.* **45c**, 455–458.

Tobin, A. K., and Rogers, W. J. (1992). In *Plant Organelles* (Tobin, A. K. ed.), Society for Experimental Biology Seminar Series, Vol. 50, Cambridge University Press, Cambridge, pp. 293–323.

Tron, T., Crimi, M., Colson, A.-M., and Degli Esposti, M. (1991). *Eur. J. Biochem.* **199**, 753–760.

Trumpower, B. L. (1990). *J. Biol. Chem.* **265**, 11409–11412.

Turowski, P. N., Armstrong, W. H., Liu, S., Brown, S. N., and Lippard, S. J. (1994). *Inorg. Chem.* **33**, 636–645.

Vanlerberghe, G. C., and McIntosh, L. (1994). *Plant Physiol.* **105**, 867–874.

Vincent, J. B., Olivier-Lilley, G. L., and Averill, B. A. (1990). *Chem. Rev.* **90**, 1447–1467.

Whelan, J., McIntosh, L., and Day, D. A. (1993). *Plant Physiol.* **103**, 1481.

Whitehouse, D. G., and Moore, A. L. (1995). In *Advances in Cellular and Molecular Biology of Plants* (Levings, C. S., and Vasil, I. K. eds.), Molecular Biology of the Mitochondria. Vol. 2, Kluwer Academic, Dordrecht, pp. 313–344.

Wilkins, R. G. (1992). *Chem. Soc. Rev.* **21**, 171–178.

Wilkins, P. C., and Dalton, H. (1994). *Biochem. Soc. Trans.* **22**, 700–704.

Wiskich, J. T., and Meidan, E. (1992). In *Plant Organelles* (Tobin, A. K., ed.), Society for Experimental Biology Seminar Series, Vol. 50, Cambridge University Press, Cambridge, pp. 1–19.